Breakthrough Platform Technology to Assess Critical Quality Attributes of Therapeutic Proteins for Enhanced Speed to Market

Belinda Pastrana[1], Sherly Nieves[1], and Curtis Meuse[2]
[1]Protein Dynamic Solutions, Inc. Wakefield, MA 01880
[2]IBBR, University of Maryland and Biomolecular Measurement Division, NIST, MD, USA

Introduction

Recent years have seen an unprecedented growth in the development of therapeutic proteins for the treatment of a wide variety of diseases. The challenges of engineering these products to optimize stability, ensure efficacy and minimize immunogenicity risk are well-known to be complex.

Analytical methodologies to assess critical quality attributes (CQAs) of therapeutic proteins are varied, time-consuming and can involve complicated sample preparation and analysis. Multiple analytical tools are routinely deployed for each CQA assessment, and the results provide limited understanding of how, and to what extent, each CQA impacts safety and efficacy. This fragmented approach contributes to the high cost, long timelines and increased risk of safety and loss of efficacy of the therapeutic candidate.

Understanding deamidation at the molecular level is critical for the development and commercialization of therapeutic proteins. Comprehensive characterization and efficient monitoring of deamidation events and their potential impact on protein stability, self-association and aggregation can effectively reduce the risk of immunogenicity. When applied within developability assessment, identification of deamidation risk can be used for sequence modification to improve biotherapeutic stability profiles. This comprehensive characterization is well suited for implementation during developability assessment for pre-clinical candidate selection.

Herein, we demonstrate the use of the ProteinMentor platform for the characterization and monitoring of deamidation using a dilution series of the NISTmAb Primary Sample (PS 8670).

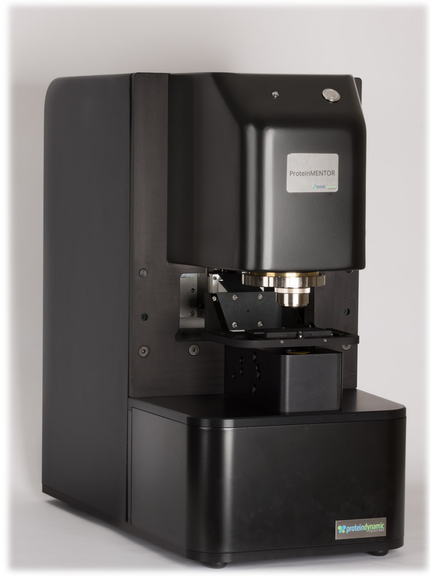

ProteinMentor is a unique combination of Quantum Cascade Laser (QCL) microscopy and spectroscopy which allows for the direct visualization of aggregates and the spectroscopic evaluation of molecular events that lead to structural changes, self-association and ultimately aggregation. We demonstrate the applicability of the platform for the assessment of deamidation.

The unique design of the microscope stage and slide cell array (SCA) allows samples to be monitored under controlled thermal conditions, with a fixed path length, which is critical for comparability while ensuring both reproducibility and accuracy.

Methods

No sample preparation steps are needed to evaluate deamidation and stability. The sample is simply diluted to generate a dilution series. A dilution series of NISTmAb (PS 8670) was prepared in 25 mM L-histidine at pH 6.0. Concentrations were 100, 70, 40, 10, 5 and 2.5 µg/µL. One µL of each sample was applied to the ProteinMentor slide cell array (SCA). The mAb samples are intact (full-length) and evaluated as such in their formulation for comparative assessment.

The SCA was then placed in a heated accessory with (+/- 0.5 °C) thermal control. Hyperspectral (HS) images were acquired within the temperature range of 28 – 60 °C with 8 °C intervals and 4 min equilibration periods using ProteinMentor. For a comparative analysis we chose a temperature range below the onset of thermal transition to establish differences in stability that would not involve thermal unfolding to the point of denaturation[1].

Each HS image is comprised of 223,000 QCL IRM spectra and takes about 40 seconds to acquire. **Figure 1**, displays a schematic with all the types of spectral analysis, resulting in the comprehensive molecular description that is obtained from a single microliter sample. This being just one of an array of samples during a comparability assessment.

Spectral analysis was performed to generate plots (**Figure 1, steps 2-6**) including both two-dimensional co-distribution spectroscopy (2D-CDS) and the two-dimensional infrared correlational spectroscopy (2D-COS) using the Correlation Dynamics™ software.

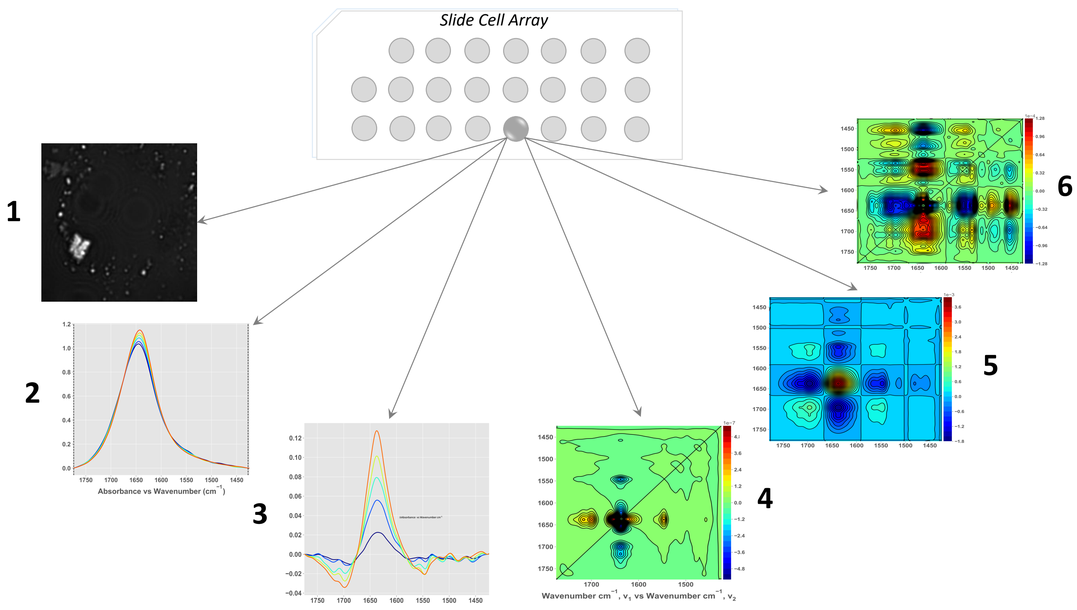

Figure 1: ProteinMentor provides a wealth of information from a single 40 second analysis in a 1 µL sample. A schematic of the slide cell array with 21 samples and 2 controls is shown at the top. For every NISTmAb concentration, a series of HS images were acquired at every set temperature.

(1) Hyperspectral images provide a visual indicator of any aggregates larger than 4.3 µm. No aggregates were seen in this study. (2) IR spectra are simply 2-point baseline corrected with no data manipulation. (3) The difference spectra show the changes that are occurring, and also remove the contribution of bulk water in the IR spectra. The spectrum at the initial set temperature is subtracted from all subsequent spectra. (4-6) A series of correlation algorithms are then applied to interrogate the data and generate the 2-D plots

Results and Discussion

The design of the ProteinMentor platform, with the QCL microscope and heated Slide Cell Array (SCA), provides an enhanced S/N with accurate thermal control and allows for the difference spectra to be generated (**Figure 1, step 3**). The difference spectra are generated by simply subtracting the first spectrum from all subsequent spectra. This allows for the subtraction of the H_2O contribution and removes any spectral contributions that did not change over the course of the thermal stress evaluation.

2D-COS was introduced during the late 1980's by Noda[2,3], and proven for the analysis of protein applications by others. The algorithm allows for the study of changes in the secondary structure of proteins as well as side chain interactions as a function of perturbation. The use of correlation plots provides enhanced resolution and selectivity of the peak intensity changes within the spectral region of interest (**Figure 1, steps 4-6**). The peak assignments have been well established for the Mid-infrared spectral region. If the protein sequence is provided, the location of the changes within the protein are also determined and deamidation can be assigned to specific amino acid(s).

Determining the extent of deamidation

The two-step chemical reactions for both asparagine and glutamine deamidation are shown in **Figure 2**. The deamidation of asparagine or glutamine residues adds a negative charge to the protein. In the case of asparagine, if the iso-aspartate product is formed, an additional carbon atom is introduced to the protein backbone, as shown in **Figure 2A**. Consequently, a deamidation event causes intensity changes for specific vibrational modes of the side chains within the protein which are monitored in real-time **(Table 1, Figure 3**). Also, the secondary structure associated vibrational modes are monitored simultaneously to evaluate the stability of the protein. The unique design of the ProteinMentor platform and SCA allows for the determination of the extent of deamidation using first principles and the known mechanisms for asparagine and glutamine deamidation. For the NISTmAb concentration series, deamidation was most apparent for glutamine within the **β**-turns of the 100 µg/µL sample.

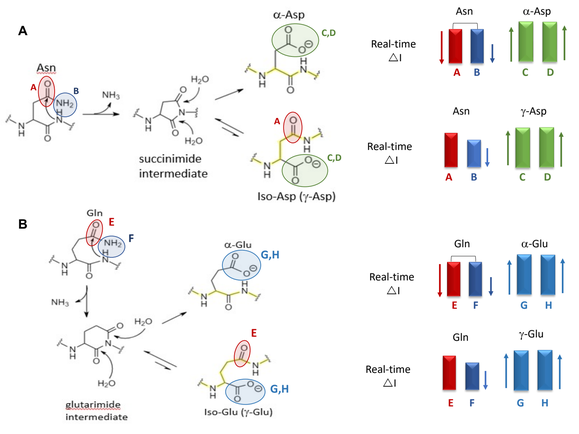

Figure 2: Schematic representing asparagine (A) and glutamine (B) deamidation and vibrational modes (for key functional groups) that are monitored to determine the extent of deamidation. Bar graphs to the right of each scheme correspond to intensity changes for the vibrational modes that are monitored in real-time during the process. The arrows define the direction and the proportionate change in intensity is determined. The change in proportion of the carbonyl and amide vibrational modes (A/B for asparagine and E/F for glutamine) designates if the product is the isoform.

Determining the site of deamidation

When the sequence is provided, the site of deamidation can also be determined. When there is a deamidation event occurring at one specific site, perturbations due to that deamidation process can be seen in neighboring residues, and within the secondary structure (**Figure 4**). The molecular order of events is determined using a set of rules established by Noda[2,3].

Concentration (µg/µL)	Residue	β turn (1696 cm⁻¹)		β turn (1681 cm⁻¹)		Hinge loop (1663 cm⁻¹)		α-helix (1653 cm⁻¹)		β sheet (1636 cm⁻¹)		Overall Extent of Deamidation	
100	N	0.33	±0.02	0.09	±0.00	0.00	±0.00	0.00	±0.00	0.00	±0.00	0.42	±0.02
	Q	1.35	±0.10	2.01	±0.24	0.00	±0.00	0.00	±0.00	0.00	±0.00	3.36	±0.26
70	N	0.54	±0.17	0.14	±0.01	0.00	±0.00	0.00	±0.00	0.00	±0.00	0.68	±0.17
	Q	0.82	±0.17	0.26	±0.05	0.00	±0.00	0.00	±0.00	0.00	±0.00	1.08	±0.18
40	N	0.26	±0.02	0.12	±0.00	0.00	±0.00	0.00	±0.00	0.00	±0.00	0.38	±0.02
	Q	0.78	±0.08	0.54	±0.04	0.00	±0.00	0.00	±0.00	0.00	±0.00	1.32	±0.09
10	N	0.10	±0.00	0.03	±0.00	0.08	±0.01	0.12	±0.01	0.10	±0.01	0.43	±0.02
	Q	0.10	±0.02	0.02	±0.01	0.00	±0.00	0.00	±0.00	0.00	±0.00	0.12	±0.02
5	N	0.16	±0.02	0.11	±0.01	0.00	±0.00	0.00	±0.00	0.00	±0.00	0.27	±0.02
	Q	0.84	±0.08	0.60	±0.05	0.00	±0.00	0.00	±0.00	0.00	±0.00	1.44	±0.09
2.5	N	0.04	±0.01	0.03	±0.00	0.01	±0.00	0.02	±0.00	0.06	±0.01	0.16	±0.01
	Q	0.17	±0.01	0.04	±0.01	0.42	±0.02	0.00	±0.00	0.00	±0.00	0.63	±0.02

Table 1: The extent of deamidation associated within each secondary structure type of the NISTmAb concentration series and the overall (summed) extent of deamidation. Each value represents the number (or fraction) of deamidation sites within each secondary structure and the overall protein. The error propagation is also included.

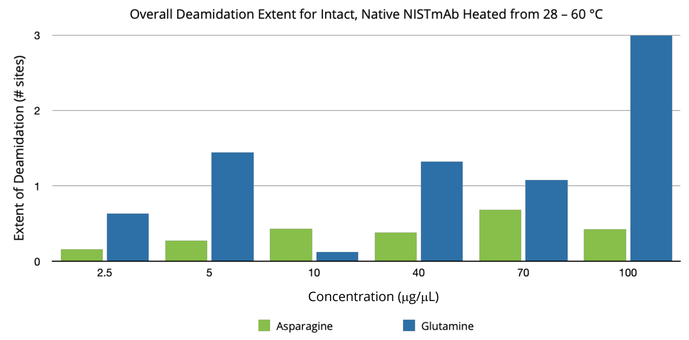

Figure 3: Bar graph of the overall extent of asparagine (green) and glutamine (blue) deamidation for the full-length, native NISTmAb as a function of concentration over the thermal ramp. The greatest risk of deamidation was apparent for glutamine in the 100 µg/µL sample.

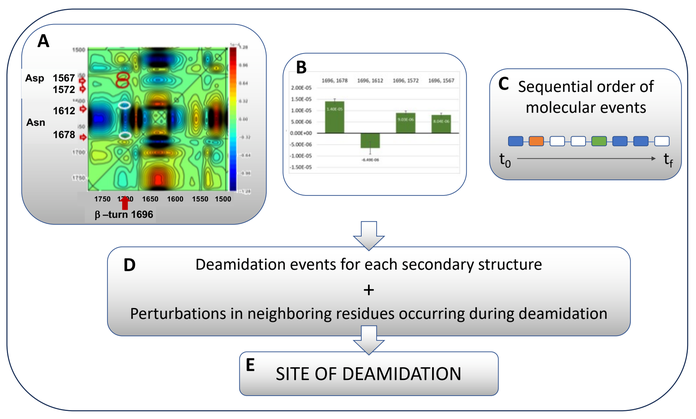

Figure 4: Schematic for the process to identify sites of deamidation using ProteinMentor and 2-D COS.

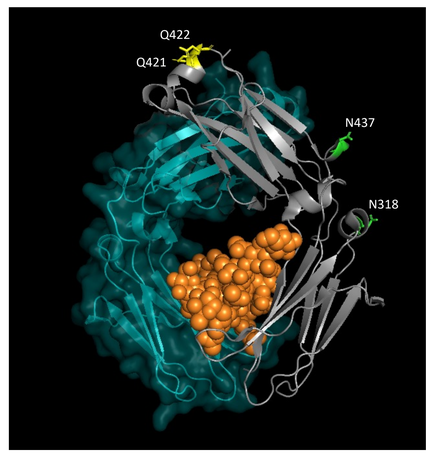

Figure 5: NISTmAb Fc high resolution structure representation (PDB ID: 5VGP), with deamidation sites labeled (green sticks) asparagine (N) and (yellow sticks) glutamine (Q)) and glycosylation shown in orange. Only one of the dimer components (dark grey) chain A, shows the deamidation site labels. All deamidation sites within the Fc HC are exposed to the aqueous environment. The model was generated using the PyMOL Molecular Graphics System, Version 2.3, Schrödinger, LLC.

Comparison with published results

The spatial location of the deamidation sites identified in this study were used for the generation of structural models from published structures for NISTmAb[4,5]. The model for the Fc region is shown in **Figure 5** and highlights the spatial location of the deamidation sites and their solvent accessibility. Overall, there was no risk of deamidation observed for the CDRs, which is a critical consideration for target binding. For NISTmAb, sites of both forced and spontaneous deamidation on asparagine and glutamine residues have been reported. The deamidation sites that were identified in the heavy chain (N318, N437 and Q421/422) and the light chain (N157, Q36 and Q154) in this study agree with published LC-MS studies by multiple groups, different instruments and different sample preparation protocols.

Conclusion

The ProteinMentor platform comparative assessment has proven to be highly effective for directly monitoring the deamidation process of full-length proteins in formulation without sample preparative steps. The comprehensive data set provides unprecedented understanding of deamidation and its impact. The ProteinMentor platform can also be used for other CQA analyses to provide multi-attribute analysis of therapeutic proteins.

References

1. Pastrana, B., Meuse, C.W., "Two-Dimensional Correlation and Two-Dimensional Co-Distribution Spectroscopies of Proteins" *Encyl. Anal. Chem.*, 29 September, 2022, Ed Meyers, R., https://doi.org/10.1002/9780470027318.a9792
2. Noda, I. Dowrey, A.E. Marcott, C. Story, G.M. Ozaki, Y. *Appl. Spectrosc.,* 2000, 54, 236A-248A. https://doi.org/10.1366/0003702001950454
3. Noda, I. J. Mol. Struct., 2016, 1124, 29e41. https://doi.org/10.1016/j.molstruc.2016.01.089
4. D.T. Gallagher, Karageorgos, I. Hudgens, J.W. Galvin, C.V. ',*Data Brief.,* 16, 29 (2018). https://doi.org/10.1016/J.DIB.2017.11.013
5. D.T. Gallagher, Connor V.G. and Karageorgos, I. *Acta Crystallogr. F Struct. Biol. Commun.,* 74, 524-529 (2018). https://doi.org/10.1107/S2053230X18009834.

NSF SBIR PII Award 1632420